

Application of Fuzzy Best Worse Multi Criteria Decision Making Method for Flood Prioritization

Sarita Gajbhiye Meshram

Ton Duc Thang University

Ali reza Ildoromi (✉ a.ildoromi@yahoo.com)

University of Malayer

Mehdi Sepehri

Yazd University

Research Article

Keywords: Flood, Prioritization, Best worse method, fuzzy

Posted Date: June 17th, 2021

DOI: <https://doi.org/10.21203/rs.3.rs-581169/v1>

License: © ⓘ This work is licensed under a Creative Commons Attribution 4.0 International License.

[Read Full License](#)

27 **1. Introduction**

28 Floods are one of the natural disasters that occur every year to global scale (Field et al., 2012).
29 In recent decades, floods are known as the main defendants of financial and life losses. Despite
30 these descriptions, there are some solutions that can be effective against reducing or preventing
31 flood events (Adhikari et al., 2010; Smith and Ward, 1998). The results of studies conducted by
32 the Forest, Rangeland and Watershed Management Organization (FRWMO) in Iran (1986-
33 2007) show that 2498 flood events were occurred and resulted in the deaths of 3299 people,
34 injuries of 1733 people, partial and complete destruction of 135092 and 1572 building units
35 (totally 136,664 damaged and destroyed buildings) (Almasi and Soltani, 2017; Hajian et al.,
36 2019; Hooshyaripor et al., 2020; Yadollahie, 2019).

37 Flood is one of the most frequent and costly hazard worldwide which impress
38 approximately 20000 lives per year (Sarhadi et al., 2012). Until to data, it is incredible to
39 prevent flood but some appropriate measures can be underpinned to somewhat compensate it
40 (Termeh et al., 2018). In scale of catchment, given the inherent complexity of formulating flood
41 risk management strategies and its high uncertainty due to some reasons such as large input
42 data and long processing time, it is necessity to select sub-watersheds as a small-scale
43 hydrological unit to prioritize them based on their flood potential (Aher et al., 2014; Anees et
44 al., 2019; Shivhare et al., 2018). In this context, there are variety of approaches available to
45 analysis and prioritize sub-watersheds using Multi Criteria Decision Analysis (MCDA) (Akay
46 and Koçyigit, 2020; Chitsaz and Banihabib, 2015; Ghaleno et al., 2020; Sepehri et al., 2019c),
47 Soil and Water Assessment Tool (SWAT) (Mishra et al., 2007; Talebi et al., 2019a), artificial
48 neural network (ANN) (Dehghanian et al., 2020), Storm Water Management Model
49 (SWMM) (Babaei et al., 2018), support vector machine (SVM) (Fan et al., 2018; Tehrani et
50 al., 2014) and The Hydrologic Modeling System (HEC-HMS) (Malekinezhad et al., 2017;
51 Talebi et al., 2019b). Among aforementioned methods, MCDA has been taking into account

52 due to its capability to handle nonlinear and complex problems and its usability to prioritize
53 ungauged watershed.

54 MCDA are most usable methods which can be used to manage large amount of data
55 and solving decision making under scale, quantitative, qualitative and conflict factors
56 (Fernández and Lutz, 2010; Mahmoud and Gan, 2018). The Analytic Hierarchy Process (AHP)
57 which was developed by Saaty (1980), due to some reasons such as cost-effective, ease to used
58 and understand has made to one of the most popular method among MCDA (Zou et al., 2013),
59 which has been successful in various natural hazard studies such as landslide (Bahrami et al.,
60 2020; Kayastha et al., 2013; Myronidis et al., 2016), flood magnitude (Lin et al., 2020; Sepehri
61 et al., 2017; Swain et al., 2020), groundwater vulnerability (Abdullah et al., 2018; Das and Pal,
62 2020; Sener and Davraz, 2013).

63 Rahmati et al. (2016) identified most susceptibility sub-watersheds to flood magnitude
64 using AHP and natural and anthropogenic factors. Mahmoud and Gan (2018) attempted to
65 prepare flood hazard mapping in arid regions of Middle East using AHP and 10 flood- related
66 factors i.e. annual rainfall, flow accumulation, distance to drainage network, elevation, slope,
67 geology, land use/cover, drainage density, soil type and runoff. In other similar study, Dash
68 and Sar (2020) used AHP to delineate flood susceptibility mapping. AHP was used to assigning
69 weights to flood-related factors based on importance role of them on flood magnitude. The
70 AHP and other similar methods is categorized as subjective or experts' knowledge-based
71 methods (Sepehri et al., 2019b; Smithson, 1989). In these methods, for assigning weights to
72 factors, it is necessity to compare factors relative to each other. The process of comparison is
73 the main source of inconsistency of these methods (Guo and Zhao, 2017). In this regard, several
74 methods were developed to reduce the number of pairwise comparisons. In recent years, a new
75 method was introduced by Rezaei (2015). This method is more optimal version of AHP with
76 the need of less compared data, causing more consistency of the results. However, the weak

77 point of the BWM is related to kind of import data. This method such as AHP, use a limited 9-
78 point table. In here, experts face to a dilemma to choice a point of initial weighting to factors
79 causing inconsistency in the results. Therefore, it is better to use fuzzy number other than
80 limited 9-point table which is more in line with actual situations and can obtain more
81 convincing ranking results (Ali and Rashid, 2019; Guo and Zhao, 2017).The sad ekbatan
82 watershed in the field if floods and its related financial and ecological losses can be regarded
83 as one of the most critical areas in central of Iran. However, there is no done comprehensive
84 and efficient works to reduce the flood consequences. Thus the main objective of this study is
85 to flood prioritization based on fuzzy- best worse multi criteria decision making method of
86 efficient prioritizing sub-watersheds.

87

88 **2. Case study**

89 The sad ekbatan with an area of 180 km² is watershed located in northern part of Hamadan
90 province, Iran. The watershed coordinates system lies between 31°24/45" to 31°27/ 29" north;
91 41°55/20" to 41°57/34" east (Fig. 1). The elevation map ranges of 1948 to 3442 meters above
92 the sea level. Based on sad ekbatan climatology data, the average annual rainfall and
93 temperature is 343.11 mm and +10.75 °C. From viewpoint of geology, the case study has
94 located in Sanandaj- Sirjan metamorphic zone which has been categorized with sedimentary
95 rock units, including Sl ‘Mb ‘Schg ‘Schan ‘Schst ‘hc ‘Schsp ‘K1s,c ‘Qt. Rangeland is one the
96 most important covers in the case study, but in two last decade due to economic and social
97 problems, this cover has been transferred to farming areas, leading to an increase of 30% in
98 rate of runoff volume (Farokhzadeh et al., 2015).

99

100 **Fig.1:** location map of the case study

101

102

103 **2. Materials and Methods**

104 The used procedural in this study, is based on studies of Hazarika et al. (2018); Sepehri et al.
105 (2019a); Arabameri et al. (2019) and Costache and Bui (2020) which can be summarized as
106 three main stages:

- 107 1. Establishing flood-related indices.
- 108 2. Applying ensemble of Fuzzy method and BWM to assigning weights to used indices based
109 on importance of them on flood magnitude.
- 110 3. Prioritization of sub-watersheds using weighted overlay method (WOM) (Fig.2).

111 **Fig.2: Flowchart of the used methodology**

112

113 **3.1 Flood-related indices**

114 The flood magnitude is a function of metrological and catchment properties which known as
115 flood-related indices (Chen et al., 2019; Fernández and Lutz, 2010; Hong et al., 2018).
116 Therefore, an acceptable flood hazard mapping is depending on quality of the spatial and
117 temporal the indices. In this study based on best of our knowledge and field surveys, five flood-
118 related indices were considered. Those factors are: entropy of drainage network (En), index of
119 connectivity (IC), stream power index (SPI), curvature (C) and curve number (CN).

120

121 **Entropy of drainage network (En):** One of the most important geomorphic indices that can
122 play a very important role in flood frequency and probability is the complexity of the drainage
123 network (Ariza-Villaverde et al., 2013; Veltri et al., 1996; Zhang et al., 2015). In most studies
124 of flood subjects, the authors use the simple features of drainage network for description of it.
125 These features such as length of drainage network, radius of drainage network curvature,
126 drainage density have not an accurate description of drainage network (Ildoromi et al., 2019;
127 Zhang et al., 2015). In recent years, a new concept as irregularity has been raised between
128 scholars to better describe the drainage network. The entropy concept, is one of the most

129 popular methods which can be used to assess the irregularity features of drainage network. To
 130 calculate entropy of drainage network, it is necessary to use box-counting algorithm. In the
 131 algorithm, the drainage network is broken down to various pixel sizes and then by using Eq. 1,
 132 the entropy of drainage network is calculated.

$$P_i = -k \sum_{j=1}^n f_{ij} \ln f_{ij} \quad (1)$$

133
 134 Where

$$f_{ij} = \frac{r_{ij}}{\sum_{j=1}^n r_{ij}}$$

$$r_{ij} = \frac{x_{ij} - \min\{x_{ij}\}}{\max\{x_{ij}\} - \min\{x_{ij}\}}$$

137
 138 **Index of connectivity (IC):** In hydrology studies, the concept of connectivity is used for
 139 description of geomorphic features (Wohl et al., 2019) and process-based dynamic researches
 140 and can be defined as degree of sediment or runoff coupling between landscape elements
 141 (Borselli et al., 2008; Heckmann et al., 2018). Sediment connectivity showing the potential
 142 moving of a special particle of source to sink to different temporal and spatial scales (Fryirs,
 143 2013; Llena et al., 2019). In order to prepare a flood hazard map with high accuracy, it is
 144 necessary to use connectivity indices.

145 In recent years, several hydrological connectivity indices have been developed to
 146 evaluate the potential for a landscape to be connected (Calsamiglia et al., 2018). On the other
 147 hand, the existence of the raster-based indices can be considered as an opportunity to assess
 148 the spatial distribution of the sediment connectivity (Llena et al., 2019). The index of
 149 connectivity which introduced by Borselli et al. (2008) is known as most popular method which
 150 has used in this study (Eq. 2).

$$IC = \log_{10} \left(\frac{Dup}{Ddn} \right) \quad (2)$$

151

152 The numerator of this equation (i.e. D_{up}) which called as upslope component, demonstrates
153 the potential of upslope of a pixel in downward routing of sediment/runoff and denominator
154 (i.e. D_{dn}) represents the flow length of the pixel has to travel to nearest sink or target (Llena et
155 al., 2019; Schopper et al., 2019). D_{up} is calculated as follows:

$$D_{up} = \bar{w}\bar{s}\sqrt{A} \quad (3)$$

156 Where \bar{w} and \bar{s} are average weighting and slope gradient (m/m) of the upslope contributing
157 area, respectively and A is upslope contributing area (m^2). The D_{dn} is computed as:

$$D_{dn} = \sum_i \frac{d_i}{w_i s_i} \quad (4)$$

158

159 Where d_i is length of the pixel (i) along downslope (m), w_i and s_i are the weight and sloe of
160 pixel (i), respectively.

161 Based on studies of Mayor et al. (2008), López-Vicente and Ben-Salem (2019), Schopper et
162 al. (2019), and Sepehri et al. (2020), we computed w_i using following equation:

$$w_i = \left(1 - \frac{(Mean\ altitude - Altitude)}{Range\ altitude} \right) \quad (5)$$

163

164 The altitude for each pixel through the case study can be extracted from DEM.

165

166 **Stream power index (SPI):** In hydrology studies, this parameter is known as bridge for
167 connection between water flow paths, flow accumulations and slope(Chen and Yu, 2011;
168 Danielson, 2013; Regmi et al., 2014). This parameter can be calculated from digital elevation
169 model (DEM) in ArcGIS10.7 using Eq. 6 (Nampak et al., 2014). At the specific point of the
170 topographic surface, the higher values of the parameter show that surface water has more
171 strength of erosive rather than lower values (Moore and Grayson, 1991).

$$SPI = A_s \tan \beta \quad (6)$$

172

173 **Curvature:** Curvature is the one of the mostly used morphometric factor which describe the
174 shape of the ground surface (Il'Inskii and Yakimov, 1987). In this study, the parameter was
175 extracting from DEM in ArcGIS 10.7. The value of the parameter varies from negative
176 (concave areas) to until positive values (convex areas). Convex are the process of runoff is
177 dominating and they are responsible for downslope flooding (Costache and Bui, 2020; Zaharia
178 et al., 2017).

179

180 **Curve number (CN):** The CN is a conceptual and empirical parameter which developed in
181 1954 by the USDA Soil Conservation Service(Rallison, 1980). This parameter is a function of
182 land use and hydrologic soil group which is used for determination of the potential runoff in
183 hydrologic engineering and environmental impact analyses (Ponce and Hawkins, 1996).

184

185 **3.2 The Proposed F-BWM Model**

186 **3.2.1 Fuzzy Sets and triangular fuzzy numbers**

187 The subjective MCDA is sensitive to experts' judgments, causing difficultly evaluating the
188 weights when the experts uses natural language such as "very better", "somewhat worse", or
189 "so much better" to express a kind of general preferences(Hafezalkotob and Hafezalkotob,
190 2017). In mathematics, these natural languages are categorized as crisp sets. The concept of
191 crisp sets only implied on full membership and non-membership, whereas in fuzzy set each
192 elements can be partially membership(Boakai, 2016; Sepehri et al., 2019c). For the first time,
193 the concept of fuzzy system was introduced and characterized using membership functions by
194 Zadeh (1965) which grading membership between 0 and 1. In decision- making problems, the
195 triangular fuzzy number (TFN) is one of the most used membership functions, which can be
196 donated to triplet (l, m, u) , where $l < m < u$ (Dong et al., 2021; Guo and Zhao, 2017).
197 The triangular fuzzy number is as follow:

$$\mu_{\tilde{A}} = \begin{cases} 0, & x < l \\ \frac{x-l}{m-l}, & l \leq x \leq m \\ \frac{u-x}{u-m}, & m \leq x \leq u \\ 0, & x \geq u \end{cases} \quad (7)$$

198 Where l, m, u are the lower, median and upper numbers of \tilde{A} (for the basic mathematical
199 calculations of two TFNs, can be referred to (Carlsson and Fullér, 2001).

200 3.2.2 Fuzzy best-worst method (F-BWM)

201 Best-worst method (BWM) proposed by Rezaei (2015) is a new subjectively MCDA which
202 can be used to derive optimal weights of criteria set $\{c_1, c_1, \dots, c_j, \dots, c_n\}$. In this content, it is
203 necessity to determine the best (e.g., the most favorable) and the worst (e.g., the least favorable)
204 of criteria by experts. Afterwards, these criteria are compared relative to each other based on
205 natural language. In F-BWM, it is necessity to transfer the natural language to fuzzy rating
206 based on rules of transformation in Table. 1 (Dong et al., 2021; Guo and Zhao, 2017). The
207 fuzzy comparison can be showed as follows:

$$\tilde{A} = \begin{bmatrix} \tilde{a}_{11} & \cdots & \tilde{a}_{1n} \\ \vdots & \ddots & \vdots \\ \tilde{a}_{n1} & \cdots & \tilde{a}_{nn} \end{bmatrix} \quad (8)$$

208 Where each element of the matrix \tilde{A} represent the relative importance of criterion i to criterion
209 j , $a_{ij} = (1,1,1)$ when $i = j$. It must be noted that in BWM method, there is no need to n fuzzy
210 performance comparison to obtain a completed matrix \tilde{A} .

211 **Table 1:** Transformation rules of natural languages to membership functions

212 In the current study, the details of F-BWM algorithm to calculate the fuzzy weights can be
213 briefly described as follow (Dong et al., 2021; Guo and Zhao, 2017):

- 214 1. Provide a set of desired criteria $\{c_1, c_1, \dots, c_j, \dots, c_n\}$
- 215 2. Determine the best (c_B) and worst (c_W) criterion
- 216 3. Provide \tilde{A}_B which shows fuzzy reference comparisons of c_B over all the criteria.

$$\tilde{A}_B = [\tilde{a}_{B1}, \tilde{a}_{B2}, \dots, \tilde{a}_{Bn}] \quad (9)$$

217 Where \tilde{a}_{Bj} is the fuzzy preference of c_B over c_j , $\tilde{a}_{Bj} = (a_{Bj}^l, a_{Bj}^m, a_{Bj}^u)$, $j=1,2,\dots,n$ and $\tilde{a}_{BB} =$
 218 $(1,1,1)$

219 4. Provide \tilde{A}_W which shows fuzzy reference comparisons of all the criteria over c_W .

$$\tilde{A}_W = [\tilde{a}_{1W}, \tilde{a}_{2W}, \dots, \tilde{a}_{nW}] \quad (10)$$

220 Where \tilde{a}_{jW} is the fuzzy preference of c_j over c_W , $\tilde{a}_{jW} = (a_{jW}^l, a_{jW}^m, a_{jW}^u)$, $j=1,2,\dots,n$ and $\tilde{a}_{WW} =$
 221 $(1,1,1)$

222 5. Determine the optimal fuzzy weight $\tilde{w}^* = [w_1^*, w_2^*, \dots, w_n^*]$, where $\tilde{w}_j^* =$
 223 $(w_j^{*l}, w_j^{*m}, w_j^{*u})$ shows the optimal fuzzy weight of c_j which is calculated using below
 224 model:

$$\min \max_j \left\{ \left| \frac{\tilde{w}_B}{\tilde{w}_j} - \tilde{a}_{Bj} \right|, \left| \frac{\tilde{w}_j}{\tilde{w}_W} - \tilde{a}_{jW} \right| \right\} \quad (11)$$

225

$$s. t. \begin{cases} \sum_{j=1}^n R(\tilde{w}_j) = 1 \\ l_j^w \leq m_j^w \leq u_j^w \\ l_j^w \geq 0 \\ j = 1, 2, \dots, n \end{cases}$$

227 Where $\tilde{w}_B = (l_B^w, m_B^w, u_B^w)$, $\tilde{w}_j = (l_j^w, m_j^w, u_j^w)$, $\tilde{w}_W = (l_W^w, m_W^w, u_W^w)$, $\tilde{a}_{Bj} =$
 228 $(l_{Bj}^w, m_{Bj}^w, u_{Bj}^w)$, $\tilde{a}_{jW} = (l_{jW}^w, m_{jW}^w, u_{jW}^w)$ and $R(\tilde{w}_j) = 1/6(w_j^l + 4w_j^m + w_j^u)$

229 The above model can be transferred as below optimization model which are based on
 230 consistency ratio (ξ) (next step).

$$\min \xi \quad (12)$$

$$s. t. \left\{ \begin{array}{l} \left| \frac{\tilde{w}_B}{\tilde{w}_j} - \tilde{a}_{Bj} \right| \leq \xi \\ \left| \frac{\tilde{w}_j}{\tilde{w}_W} - \tilde{a}_{jW} \right| \leq \xi \\ \sum_{j=1}^n R(\tilde{w}_j) = 1 \\ l_j^w \leq m_j^w \leq u_j^w \\ l_j^w \geq 0 \\ j = 1, 2, \dots, n \end{array} \right.$$

231 Where $\tilde{\xi} = (l^\xi, m^\xi, u^\xi)$ and it can be assumed that $\tilde{\xi}^* = (k^*, k^*, k^*) \leq l^\xi$, then Eq. 12 can be
 232 transferred as:

$$\begin{array}{l} \min \tilde{\xi}^* \\ s. t. \left\{ \begin{array}{l} \left| \frac{(l_B^w, m_B^w, u_B^w)}{(l_j^w, m_j^w, u_j^w)} - (l_{Bj}, m_{Bj}, u_{Bj}) \right| \leq (k^*, k^*, k^*) \\ \left| \frac{(l_j^w, m_j^w, u_j^w)}{(l_W^w, m_W^w, u_W^w)} - (l_{jW}, m_{jW}, u_{jW}) \right| \leq (k^*, k^*, k^*) \\ \sum_{j=1}^n R(\tilde{w}_i) = 1 \\ l_j^w \leq m_j^w \leq u_j^w \\ l_j^w \geq 0 \\ j = 1, 2, \dots, n \end{array} \right. \end{array} \quad (13)$$

233

234 By solving above model, the optimal fuzzy weight $(\tilde{w}_1^*, \tilde{w}_2^*, \dots, \tilde{w}_n^*)$ can be calculated.

235 6. Determine the consistency ratio using Eq. 14 and Table. 2 (its calculation is same as

236 BWM (refer to Rezaei (2015)).

$$\begin{aligned} \xi^2 - (1 + 2\tilde{a}_{BW})\xi + (\tilde{a}_{BW}^2 - \tilde{a}_{BW}) &= 0, \text{ Consistency ratio} \\ &= \frac{\xi^*}{\text{consistency index}} \end{aligned} \quad (14)$$

237

238 **Table 2:** Consistency index (CI) values.

239

240

241 **3.2.3 Removing scales of raster flood related- criteria**

242 **3.2.3.1 Transforming values of raster flood related- criteria to specific value**

243 The F-BWM is related to importance of criteria related to each other. It is obvious that the
244 internal values of each criterion have difference importance of flood degree which must be
245 considered. Also, apart En and CN criteria, the all used flood-related criteria are raster file
246 (current format of ArcGIS10.7). In order to prioritize sub-watershed, it is necessity to transform
247 raster file to a specific value which is proxy of flooding degree. To do this, the below algorithm
248 was used.

- 249 • Reclassify the values of raster criteria for each sub-watershed

250 Each sub-catchment was divided into five clusters based on the IC values. To this end, a
251 classification table was first prepared. The table's interval values were obtained from a sub-
252 catchment which has maximum standard deviation (SD). On the other hand, the table's
253 boundary values, i.e. the minimum and maximum values of the table, were estimated based on
254 the minimum and maximum IC values across all sub-catchments.

- 255 • Assigning a specific value of each sub-watershed

256 A specific value was assigned to each sub-catchment. To this end, BWM was used for pairwise
257 comparisons and ranking was assigned to each class (κ_{ij}) based on the flooding degree by each
258 IC class, in that the sediment production rate increases with increasing these indices (**Table**
259 **3**). Then, a specific value of H_i was assigned to each sub-catchment using Eq. 15.

$$H_i = \sum_{j=1}^5 \kappa_{ij} * x_{ij} \quad (15)$$

260
261 Where x_{ij} represents the area of under different classes raster criteria (stage 1) rather than total
262 area of case study, and index i and j are sub-watershed number and degree of IC (i.e., very low
263 ($j=1$), low ($j=2$), moderate ($j=3$), high ($j=4$) and very high ($j=5$)).

- 264 • Determination of inter-criteria weighting

265 The F-BWM is related to importance of criteria relative to each other. It is obvious that the
 266 internal values of each criterion have difference importance of flood degree which must be
 267 considered. After previous stage, since all used criteria (both raster and vector criteria) had
 268 direct relationship of flood degree, the Eq. 16 was used to rescale all criteria which shows the
 269 inter-criteria weighting.

$$R(w_{Hi}) = \frac{H_i - \text{Min}(H_{i=1:32})}{\text{Max}(H_{i=1:32}) - \text{Min}(H_{i=1:32})} \quad (16)$$

270

271 **3.3 Weighted overlay method (WOM)**

272 After assigning outer and inner criteria weighting, it is necessity to combination of both weights
 273 to obtain flood hazard degree for each sub-watershed. In this study, to do this, the method of
 274 WOM due to having replacement property, was used (Eq. 17)(Raj and Shaji, 2017; Sepehri et
 275 al., 2020; Thapa et al., 2017). In the property, the lower weights of some criteria can be
 276 compensated for another criterion that has a higher weight.

$$277 FH_{i=1:32} = R(\tilde{w}_j) * R(w_{Hi}) \quad (17)$$

278

279 **4. Results**

280 The statistical analysis of F-BWM has been used to prioritize sub-watersheds based on degree
 281 of flood hazard. In this regard, five flood-related criteria i.e. entropy of drainage network (C1),
 282 index of connectivity (C2), stream power index (C3), curvature (C4) and curve number (C5)
 283 were used. Based on experts' knowledge and field survey, the entropy of drainage network (c1)
 284 and curve number (c5) is considered as the best and worst criteria. Next, the fuzzy preferences
 285 to best criterion over other criteria (vector \tilde{A}_B) and all criteria over worst criteria (vector \tilde{A}_W)
 286 was determined. Then, based on step 5, the optimal fuzzy weight can be done to obtain the
 287 weights.

288

$$\min \xi^*$$

$$\begin{array}{l}
289 \\
s. t. \left\{ \begin{array}{l}
\left| \frac{(l_1^w, m_1^w, u_1^w)}{(l_5^w, m_5^w, u_5^w)} - (l_{15}, m_{15}, u_{15}) \right| \leq (k^*, k^*, k^*) \\
\left| \frac{(l_1^w, m_1^w, u_1^w)}{(l_4^w, m_4^w, u_4^w)} - (l_{14}, m_{14}, u_{14}) \right| \leq (k^*, k^*, k^*) \\
\left| \frac{(l_1^w, m_1^w, u_1^w)}{(l_3^w, m_3^w, u_3^w)} - (l_{13}, m_{13}, u_{13}) \right| \leq (k^*, k^*, k^*) \\
\vdots \\
\left| \frac{(l_5^w, m_5^w, u_5^w)}{(l_1^w, m_1^w, u_1^w)} - (l_{55}, m_{55}, u_{55}) \right| \leq (k^*, k^*, k^*) \\
\left| \frac{(l_4^w, m_4^w, u_4^w)}{(l_1^w, m_1^w, u_1^w)} - (l_{45}, m_{45}, u_{45}) \right| \leq (k^*, k^*, k^*) \\
\left| \frac{(l_3^w, m_3^w, u_3^w)}{(l_1^w, m_1^w, u_1^w)} - (l_{35}, m_{35}, u_{35}) \right| \leq (k^*, k^*, k^*)
\end{array} \right.
\end{array}$$

290 The above nonlinearity optimization problem can be transferred as crisp values, as follow:

$$291 \quad \min k^*$$

$$\begin{array}{l}
292 \\
s. t. \left\{ \begin{array}{l}
l_1 - 4 * u_5 \leq k; l_1 - 4 * u_5 \geq -k \\
m_1 - 5 * m_5 \leq k; m_1 - 5 * m_5 \geq -k \\
u_1 - 6 * l_5 \leq k; u_1 - 6 * l_5 \geq -k \\
l_1 - 3 * u_4 \leq k; l_1 - 3 * u_4 \geq -k \\
m_1 - 4 * m_4 \leq k; m_1 - 4 * m_4 \geq -k \\
u_1 - 5 * l_4 \leq k; u_1 - 5 * l_4 \geq -k \\
\vdots \\
l_4 - 1 * u_1 \leq k; l_4 - 1 * u_1 \geq -k \\
m_4 - 2 * m_1 \leq k; m_4 - 2 * m_1 \geq -k \\
u_4 - 3 * l_1 \leq k; u_4 - 3 * l_1 \geq -k \\
l_3 - 2 * u_1 \leq k; l_3 - 2 * u_1 \geq -k \\
m_3 - 3 * m_1 \leq k; m_3 - 3 * m_1 \geq -k \\
u_3 - 4 * l_1 \leq k; u_3 - 4 * l_1 \geq -k \\
\frac{1}{6} * l_1 + \frac{1}{6} * 4 * m_1 + \frac{1}{6} * u_1 + \dots + \\
\frac{1}{6} * l_5 + \frac{1}{6} * 4 * m_5 + \frac{1}{6} * u_5 = 1 \\
l_1 \geq m_1 \geq u_1; \dots; l_5 \geq m_5 \geq u_5 \\
l_1 \geq 0; \dots, l_5 \geq 0 \\
k \geq 0
\end{array} \right.
\end{array}$$

293 By solving above optimization problem, the weights of used flood-related criteria were
294 determined.

$$\begin{aligned} \tilde{w}_1^* &= (0.32, 0.42, 0.48); \tilde{w}_2^* = (0.32, 0.24, 0.20); \tilde{w}_3^* = (0.18, 0.16, 0.15); \tilde{w}_4^* = \\ &(0.09, 0.12, 0.12); \tilde{w}_5^* = (0.06, 0.07, 0.09); \tilde{\xi}^* = (0.045, 0.045, 0.045) \end{aligned}$$

297

298 *4.1 Analysis of inter-criteria weighting*

299 In order to determine the entropy (EN) for each of the 31 sub-watersheds, a box counting
 300 method was used, with the size of boxes being about 0.08 mm × 0.08 mm until 168.66mm ×
 301 168.66 mm. Then, the number of boxes in which the river network was present was calculated.
 302 Finally, the EN criterion values of each sub-watershed were determined with respect to the
 303 changes in counting of boxes (Fig. 3). The final results show that the sub-watershed 5 has the
 304 highest EN value (1.4) among other sub-watersheds. According to Fig. 1, the drainage network
 305 of this sub-watershed has the greatest branch and complexity. After calculating EN values of
 306 each sub-watershed, the all values were rescaled by using Eq. 16 which shows the inter-criteria
 307 weighting for each sub-watershed (Table 4).

308

309 **Fig. 3a:** doing algorithm of box-counting method and,b: calculating EN based on box-
 310 counting method

311

312 For calculating the inter-criteria weighting for IC, SPI and curvature criteria, the algorithm
 313 which was mentioned in section 4.3, was used. For example in IC criterion, after calculating
 314 the IC for each sub-watershed (Fig. 4), the results showed that the sub-watershed 29 has the
 315 maximum value of SD (0.91) and the other and the sub-watersheds 13(-1.65)and 20 (-
 316 10.86) have the maximum and minimum values of IC through all sub-watersheds. Therefore,
 317 for preparing the classification table to reclassify values of IC for each sub-watershed, the
 318 values of sub-watershed 29 were used for internal values of classification table and maximum
 319 and minimum values of IC regarding IC index were used for boundary conditions of
 320 classification table(Fig. 4). The IC classification table can be shown as very low (-10.85 to -

321 7.19), low (-7.19 to -6.19), moderate (-6.19 to -5.40), high (-5.40 to -4.65) and very high (-4.65
 322 to -1.57). After classifying the values of IC into five degrees of IC, a special weight using
 323 BWM method which varies from 0.06 and 0.41 was assigned to each class based on importance
 324 of it on rate of flooding degree and then by using Eqs. 15 and 16, final weight if IC for each
 325 sub-watershed was determined (the process of weighting of curvature and SPI is similar to IC
 326 (Tables 5: 7). Regarding CN criterion, the value of CN for each sub-watershed which was
 327 prepared for general department of natural resources of Hamadan province by using Eq. 16,
 328 the final weight for each sub-watershed was determined.

329
 330 **Fig. 4: IC Values for sub-watersheds**

331 Table 4: Assigning inter-criteria weighting to EN index

332 Table 5: Assigning inter/outer-criteria weighting to IC index

333 Table 6: Assigning inter/outer-criteria weighting to curvature index

334
 335 **4.2 Flood magnitude prioritization**

336 After calculating the weights of criteria, the flood prioritization was provided by integration of
 337 criteria in WOM method (Fig. 5).

338
$$FH_{i=1:32} = R_{EN}(\tilde{w}_j) * R_{EN}(w_{Hi}) + R_{IC}(\tilde{w}_j) * R_{IC}(w_{Hi}) + R_{SPI}(\tilde{w}_j) * R_{SPI}(w_{Hi}) + R_{CU}(\tilde{w}_j)$$

 339
$$* R_{CU}(w_{Hi}) + R_{CN}(\tilde{w}_j) * R_{CN}(w_{Hi})$$

340
 341 **5. Discussion**

342 In watershed scale, the sub-watersheds based on their morphometric and hydrologic properties
 343 have different hydrological behavior regarding flood degree, erosion and sedimentation.
 344 Therefore, prioritization of sub-watershed is known as crucial step for watershed management
 345 strategies. Subjective MCDA is mostly used methods for flood prioritization. These methods
 346 based on Smithson (2012) are categorized as knowledge-based methods, so that the results of

347 desired study are function of experts' decision, leading to high uncertainty of results. In this
348 regard, BWM can be used as efficiency method to reduce the number of experts' decision
349 (Rezaei, 2015). However, the existence of qualitative judgments on BWM (i.e. 9-point table)
350 can be considered as one of the main sources of uncertainty in this method, therefore, in this
351 study we used TFN to nearly resolve the drawback of qualitative judgments (Bellman and
352 Zadeh, 1970; Guo and Zhao, 2017; Zhao and Guo, 2014, 2015).

353 Fig. 4 shows the results of F-BWM in flood prioritization. Based on the figure, the land
354 used of sub-watershed 14 is composed as rock and rangeland III, leading to high value of CN,
355 IC. Also, on the other hand the drainage network of the sub-watershed has the maximum
356 entropy value of all sub-watersheds. On the contrary, the sub-watershed 15 has located in final
357 rank of flood prioritization. In this sub-watershed due to existence of straight drainage
358 networks, the value of the entropy of drainage network as most flood-related criteria has located
359 in minimum level.

360

361 **6. Conclusion**

362 In the current study, five flood-related criteria i.e. EN, IC, CN, curvature and SPI were used to
363 flood prioritization in the case study. In this regard, F-BWM as knowledge-based method was
364 used to assigning initial weights to criteria and combination them to earn flood degree. The
365 conclusion can be drawn that the EN is the most important flood-related criterion, so that the
366 sub-watershed 14 and 21 which have most and least rank of flooding degree, have the
367 maximum and minimum value of EN. In flood studies, in spite of flood degree, the main other
368 point which must be considered is related to consequences of flood events which known as
369 flood risk. In this state, the critical sub-watersheds can be better recognized for doing watershed
370 management strategies.

371

372 **Funding:** Not Applicable

373 **Data availability:** The datasets used and/or analyzed during the current study are available
374 from the corresponding author on reasonable request.

375 **Compliance with ethical standards**

376 **Ethics approval and consent to participate:** Not applicable.

377 **Consent for publication:** Not applicable.

378 **Competing interests:** The authors declare that they have no competing interests.

379 **References**

- 380 Abdullah, T.O., Ali, S.S., Al-Ansari, N.A., Knutsson, S., 2018. Possibility of Groundwater Pollution in
381 Halabja Saidu Hydrogeological Basin, Iraq Using Modified DRASTIC Model Based on AHP and
382 Tritium Isotopes. *Geosciences* 8, 236.
- 383 Adhikari, P., Hong, Y., Douglas, K.R., Kirschbaum, D.B., Gourley, J., Adler, R., Brakenridge, G.R., 2010.
384 A digitized global flood inventory (1998–2008): compilation and preliminary results. *Natural Hazards*
385 55, 405-422.
- 386 Aher, P., Adinarayana, J., Gorantiwar, S., 2014. Quantification of morphometric characterization and
387 prioritization for management planning in semi-arid tropics of India: a remote sensing and GIS
388 approach. *Journal of Hydrology* 511, 850-860.
- 389 Akay, H., Koçyiğit, M.B., 2020. Flash flood potential prioritization of sub-basins in an ungauged basin
390 in Turkey using traditional multi-criteria decision-making methods. *Soft Computing*, 1-13.
- 391 Ali, A., Rashid, T., 2019. Hesitant fuzzy best-worst multi-criteria decision-making method and its
392 applications. *International Journal of Intelligent Systems* 34, 1953-1967.
- 393 Almasi, P., Soltani, S., 2017. Assessment of the climate change impacts on flood frequency (case study:
394 Bazoft Basin, Iran). *Stochastic Environmental Research and Risk Assessment* 31, 1171-1182.
- 395 Anees, M.T., Abdullah, K., Nawawi, M., A. Rahman, N.N.N., Ismail, A.Z., Syakir, M., Abdul Kadir, M.O.,
396 2019. Prioritization of Flood Vulnerability Zones Using Remote Sensing and GIS for Hydrological
397 Modelling. *Irrigation and Drainage* 68, 176-190.
- 398 Arabameri, A., Rezaei, K., Cerdà, A., Conoscenti, C., Kalantari, Z., 2019. A comparison of statistical
399 methods and multi-criteria decision making to map flood hazard susceptibility in Northern Iran.
400 *Science of the Total Environment* 660, 443-458.
- 401 Ariza-Villaverde, A., Jiménez-Hornero, F., de Ravé, E.G., 2013. Multifractal analysis applied to the study
402 of the accuracy of DEM-based stream derivation. *Geomorphology* 197, 85-95.
- 403 Babaei, S., Ghazavi, R., Erfanian, M., 2018. Urban flood simulation and prioritization of critical urban
404 sub-catchments using SWMM model and PROMETHEE II approach. *Physics and Chemistry of the Earth,*
405 *Parts A/B/C* 105, 3-11.
- 406 Bahrami, Y., Hassani, H., Maghsoudi, A., 2020. Landslide susceptibility mapping using AHP and fuzzy
407 methods in the Gilan province, Iran. *GeoJournal*, 1-20.
- 408 Bellman, R.E., Zadeh, L.A., 1970. Decision-making in a fuzzy environment. *Management science* 17, B-
409 141-B-164.
- 410 Boakai, S., 2016. A fuzzy best-worst multi-criteria decision-making method for third-party logistics
411 provider selection.
- 412 Borselli, L., Cassi, P., Torri, D., 2008. Prolegomena to sediment and flow connectivity in the landscape:
413 a GIS and field numerical assessment. *Catena* 75, 268-277.

414 Calsamiglia, A., Fortesa, J., García-Comendador, J., Lucas-Borja, M.E., Calvo-Cases, A., Estrany, J., 2018.
415 Spatial patterns of sediment connectivity in terraced lands: Anthropogenic controls of catchment
416 sensitivity. *Land Degradation & Development* 29, 1198-1210.

417 Carlsson, C., Fullér, R., 2001. On possibilistic mean value and variance of fuzzy numbers. *Fuzzy sets and*
418 *systems* 122, 315-326.

419 Chen, C.-Y., Yu, F.-C., 2011. Morphometric analysis of debris flows and their source areas using GIS.
420 *Geomorphology* 129, 387-397.

421 Chen, W., Hong, H., Li, S., Shahabi, H., Wang, Y., Wang, X., Ahmad, B.B., 2019. Flood susceptibility
422 modelling using novel hybrid approach of reduced-error pruning trees with bagging and random
423 subspace ensembles. *Journal of Hydrology* 575, 864-873.

424 Chitsaz, N., Banihabib, M.E., 2015. Comparison of different multi criteria decision-making models in
425 prioritizing flood management alternatives. *Water Resources Management* 29, 2503-2525.

426 Costache, R., Bui, D.T., 2020. Identification of areas prone to flash-flood phenomena using multiple-
427 criteria decision-making, bivariate statistics, machine learning and their ensembles. *Science of The*
428 *Total Environment* 712, 136492.

429 Danielson, T., 2013. Utilizing a high resolution Digital Elevation Model (DEM) to develop a Stream
430 Power Index (SPI) for the Gilmore creek watershed in Winona County, Minnesota. *Papers in resource*
431 *analysis* 15.

432 Das, B., Pal, S.C., 2020. Assessment of groundwater vulnerability to over-exploitation using MCDA,
433 AHP, fuzzy logic and novel ensemble models: a case study of Goghat-I and II blocks of West Bengal,
434 India. *Environmental Earth Sciences* 79, 1-16.

435 Dash, P., Sar, J., 2020. Identification and validation of potential flood hazard area using GIS-based
436 multi-criteria analysis and satellite data-derived water index. *Journal of Flood Risk Management*.

437 Dehghanian, N., Saeid Mousavi Nadoushani, S., Saghafian, B., Damavandi, M.R., 2020. Evaluation of
438 coupled ANN-GA model to prioritize flood source areas in ungauged watersheds. *Hydrology Research*
439 51, 423-442.

440 Dong, J., Wan, S., Chen, S.-M., 2021. Fuzzy best-worst method based on triangular fuzzy numbers for
441 multi-criteria decision-making. *Information Sciences* 547, 1080-1104.

442 Fan, J., Li, M., Guo, F., Yan, Z., Zheng, X., Zhang, Y., Xu, Z., Wu, F., 2018. Priorization of River Restoration
443 by Coupling Soil and Water Assessment Tool (SWAT) and Support Vector Machine (SVM) Models in
444 the Taizi River Basin, Northern China. *International journal of environmental research and public*
445 *health* 15, 2090.

446 Farokhzadeh, B., Ildoromi, A., Attaeian, B., Nourouzi, M., 2015. Assessment the estimation of
447 suspended load under the influence of land use change using SWAT model (Case study: Yalfan
448 watershed). *Environmental Erosion Research Journal* 5, 28-46.

449 Fernández, D., Lutz, M., 2010. Urban flood hazard zoning in Tucumán Province, Argentina, using GIS
450 and multicriteria decision analysis. *Engineering Geology* 111, 90-98.

451 Field, C.B., Barros, V., Stocker, T.F., Dahe, Q., 2012. Managing the risks of extreme events and disasters
452 to advance climate change adaptation: special report of the intergovernmental panel on climate
453 change. Cambridge University Press.

454 Fryirs, K., 2013. (Dis) Connectivity in catchment sediment cascades: a fresh look at the sediment
455 delivery problem. *Earth Surface Processes and Landforms* 38, 30-46.

456 Ghaleno, M.R.D., Meshram, S.G., Alvandi, E., 2020. Pragmatic approach for prioritization of flood and
457 sedimentation hazard potential of watersheds. *Soft Computing*, 1-14.

458 Guo, S., Zhao, H., 2017. Fuzzy best-worst multi-criteria decision-making method and its applications.
459 *Knowledge-Based Systems* 121, 23-31.

460 Hafezalkotob, A., Hafezalkotob, A., 2017. A novel approach for combination of individual and group
461 decisions based on fuzzy best-worst method. *Applied Soft Computing* 59, 316-325.

462 Hajian, F., Dykes, A.P., Cavanagh, S., 2019. Assessment of the flood hazard arising from land use
463 change in a forested catchment in northern Iran. *Journal of flood risk management* 12, e12481.

464 Hazarika, N., Barman, D., Das, A., Sarma, A., Borah, S., 2018. Assessing and mapping flood hazard,
465 vulnerability and risk in the Upper Brahmaputra River valley using stakeholders' knowledge and
466 multicriteria evaluation (MCE). *Journal of Flood Risk Management* 11, S700-S716.

467 Heckmann, T., Cavalli, M., Cerdan, O., Foerster, S., Javaux, M., Lode, E., Smetanová, A., Vericat, D.,
468 Brardinoni, F., 2018. Indices of sediment connectivity: opportunities, challenges and limitations. *Earth-*
469 *Science Reviews* 187, 77-108.

470 Hong, H., Tsangaratos, P., Ilia, I., Liu, J., Zhu, A.-X., Chen, W., 2018. Application of fuzzy weight of
471 evidence and data mining techniques in construction of flood susceptibility map of Poyang County,
472 China. *Science of the total environment* 625, 575-588.

473 Hooshyaripor, F., Faraji-Ashkavar, S., Koohyian, F., Tang, Q., Noori, R., 2020. Annual flood damage
474 influenced by El Niño in the Kan River basin, Iran. *Natural Hazards and Earth System Sciences* 20, 2739-
475 2751.

476 Il'Inskii, N., Yakimov, N., 1987. Determination of the shape of the downstream slope of an earth-fill
477 dam from the seepage strength conditions at the face. *Fluid Dynamics* 22, 414-419.

478 Ildoromi, A.R., Sepehri, M., Malekinezhad, H., Kiani-Harchegani, M., Ghahramani, A., Hosseini, S.Z.,
479 Artimani, M.M., 2019. Application of Multi-Criteria Decision Making and GIS for Check Dam Layout in
480 the Ilanlu Basin, Northwest of Hamadan Province, Iran. *Physics and Chemistry of the Earth, Parts*
481 *A/B/C*.

482 Kayastha, P., Dhital, M.R., De Smedt, F., 2013. Application of the analytical hierarchy process (AHP) for
483 landslide susceptibility mapping: a case study from the Tinau watershed, west Nepal. *Computers &*
484 *Geosciences* 52, 398-408.

485 Lin, K., Chen, H., Xu, C.-Y., Yan, P., Lan, T., Liu, Z., Dong, C., 2020. Assessment of flash flood risk based
486 on improved analytic hierarchy process method and integrated maximum likelihood clustering
487 algorithm. *Journal of Hydrology* 584, 124696.

488 Llena, M., Vericat, D., Cavalli, M., Crema, S., Smith, M., 2019. The effects of land use and topographic
489 changes on sediment connectivity in mountain catchments. *Science of the Total Environment* 660,
490 899-912.

491 López-Vicente, M., Ben-Salem, N., 2019. Computing structural and functional flow and sediment
492 connectivity with a new aggregated index: A case study in a large Mediterranean catchment. *Science*
493 *of the Total Environment* 651, 179-191.

494 Mahmoud, S.H., Gan, T.Y., 2018. Multi-criteria approach to develop flood susceptibility maps in arid
495 regions of Middle East. *Journal of cleaner production* 196, 216-229.

496 Malekinezhad, H., Talebi, A., Ilderomi, A.R., Hosseini, S.Z., Sepehri, M., 2017. Flood hazard mapping
497 using fractal dimension of drainage network in Hamadan City, Iran. *Journal of Environmental*
498 *Engineering and Science* 12, 86-92.

499 Mayor, Á.G., Bautista, S., Small, E.E., Dixon, M., Bellot, J., 2008. Measurement of the connectivity of
500 runoff source areas as determined by vegetation pattern and topography: A tool for assessing
501 potential water and soil losses in drylands. *Water Resources Research* 44.

502 Mishra, A., Kar, S., Singh, V., 2007. Prioritizing structural management by quantifying the effect of land
503 use and land cover on watershed runoff and sediment yield. *Water Resources Management* 21, 1899-
504 1913.

505 Moore, I.D., Grayson, R.B., 1991. Terrain-based catchment partitioning and runoff prediction using
506 vector elevation data. *Water Resources Research* 27, 1177-1191.

507 Myronidis, D., Papageorgiou, C., Theophanous, S., 2016. Landslide susceptibility mapping based on
508 landslide history and analytic hierarchy process (AHP). *Natural Hazards* 81, 245-263.

509 Nampak, H., Pradhan, B., Abd Manap, M., 2014. Application of GIS based data driven evidential belief
510 function model to predict groundwater potential zonation. *Journal of Hydrology* 513, 283-300.

511 Ponce, V.M., Hawkins, R.H., 1996. Runoff curve number: Has it reached maturity? *Journal of hydrologic*
512 *engineering* 1, 11-19.

513 Rahmati, O., Haghizadeh, A., Stefanidis, S., 2016. Assessing the accuracy of GIS-based analytical
514 hierarchy process for watershed prioritization; Gorganrood River Basin, Iran. *Water resources*
515 *management* 30, 1131-1150.

516 Raj, D., Shaji, E., 2017. Fluoride contamination in groundwater resources of Alleppey, southern India.
517 *Geoscience Frontiers* 8, 117-124.

518 Rallison, R.E., 1980. Origin and evolution of the SCS runoff equation, Symposium on watershed
519 management 1980. ASCE, pp. 912-924.

520 Regmi, A.D., Devkota, K.C., Yoshida, K., Pradhan, B., Pourghasemi, H.R., Kumamoto, T., Akgun, A.,
521 2014. Application of frequency ratio, statistical index, and weights-of-evidence models and their
522 comparison in landslide susceptibility mapping in Central Nepal Himalaya. *Arabian Journal of*
523 *Geosciences* 7, 725-742.

524 Rezaei, J., 2015. Best-worst multi-criteria decision-making method. *Omega* 53, 49-57.

525 Saaty, T., 1980. *The Analytic Hierarchy Process*; New York, NY, McGraw Hill, reprinted by RWS
526 Publication, Pittsburgh.

527 Sarhadi, A., Soltani, S., Modarres, R., 2012. Probabilistic flood inundation mapping of ungauged rivers:
528 Linking GIS techniques and frequency analysis. *Journal of Hydrology* 458, 68-86.

529 Schopper, N., Mergili, M., Frigerio, S., Cavalli, M., Poepl, R., 2019. Analysis of lateral sediment
530 connectivity and its connection to debris flow intensity patterns at different return periods in the Fella
531 River system in northeastern Italy. *Science of The Total Environment* 658, 1586-1600.

532 Sener, E., Davraz, A., 2013. Assessment of groundwater vulnerability based on a modified DRASTIC
533 model, GIS and an analytic hierarchy process (AHP) method: the case of Egirdir Lake basin (Isparta,
534 Turkey). *Hydrogeology Journal* 21, 701-714.

535 Sepehri, M., Ildoromi, A.R., Malekinezhad, H., Ghahramani, A., Ekhtesasi, M.R., Cao, C., Kiani-
536 Harchegani, M., 2019a. Assessment of check dams' role in flood hazard mapping in a semi-arid
537 environment. *Geomatics, Natural Hazards and Risk* 10, 2239-2256.

538 Sepehri, M., Ildoromi, A.R., Malekinezhad, H., Hosseini, S.Z., Talebi, A., Goodarzi, S., 2017. Flood hazard
539 mapping for the gonbad chi region, Iran. *Journal of Environmental Engineering and Science* 12, 16-24.

540 Sepehri, M., Malekinezhad, H., Hosseini, S.Z., Ildoromi, A.R., 2019b. Assessment of flood hazard
541 mapping in urban areas using entropy weighting method: a case study in Hamadan city, Iran. *Acta*
542 *Geophysica* 67, 1435-1449.

543 Sepehri, M., Malekinezhad, H., Hosseini, S.Z., Ildoromi, A.R., 2019c. Suburban flood hazard mapping
544 in Hamadan city, Iran, *Proceedings of the Institution of Civil Engineers-Municipal Engineer*. Thomas
545 Telford Ltd, pp. 1-13.

546 Sepehri, M., Malekinezhad, H., Jahanbakhshi, F., Ildoromi, A.R., Chezgi, J., Ghorbanzadeh, O.,
547 Naghipour, E., 2020. Integration of interval rough AHP and fuzzy logic for assessment of flood prone
548 areas at the regional scale. *Acta Geophysica*.

549 Shivhare, N., Rahul, A.K., Omar, P.J., Chauhan, M.S., Gaur, S., Dikshit, P.K.S., Dwivedi, S.B., 2018.
550 Identification of critical soil erosion prone areas and prioritization of micro-watersheds using
551 geoinformatics techniques. *Ecological Engineering* 121, 26-34.

552 Smith, K., Ward, R., 1998. Mitigating and managing flood losses. *Floods: Physical Processes and Human*
553 *Impacts* (Chichester: John Wiley & Sons).

554 Smithson, M., 1989. *Cognitive Science. Ignorance and uncertainty: Emerging paradigms*. New York,
555 NY, US. Springer-Verlag Publishing. [http://dx. doi. org/10.1007/978-1-4612-3628-3](http://dx.doi.org/10.1007/978-1-4612-3628-3).

556 Smithson, M., 2012. *Ignorance and uncertainty: emerging paradigms*. Springer Science & Business
557 Media.

558 Swain, K.C., Singha, C., Nayak, L., 2020. Flood Susceptibility Mapping through the GIS-AHP Technique
559 Using the Cloud. *ISPRS International Journal of Geo-Information* 9, 720.

560 Talebi, A., Abyari, E., Parvizi, S., 2019a. Prioritization of Sub-Watersheds from Flooding Viewpoint
561 Using the SWAT Model (Arazkoose Watershed, Golestan Province). *JWSS-Isfahan University of*
562 *Technology* 23, 409-419.

563 Talebi, A., ESLAMI, Z., Abbasi, A., 2019b. Comparing prioritization from flooding of sub-basins using
564 HEC-HMS model and experimental methods in Eskandari Watershed.

565 Tehrany, M.S., Pradhan, B., Jebur, M.N., 2014. Flood susceptibility mapping using a novel ensemble
566 weights-of-evidence and support vector machine models in GIS. *Journal of hydrology* 512, 332-343.

567 Termeh, S.V.R., Kornejady, A., Pourghasemi, H.R., Keesstra, S., 2018. Flood susceptibility mapping
568 using novel ensembles of adaptive neuro fuzzy inference system and metaheuristic algorithms.
569 *Science of the Total Environment* 615, 438-451.

570 Thapa, R., Gupta, S., Reddy, D., 2017. Application of geospatial modelling technique in delineation of
571 fluoride contamination zones within Dwarka Basin, Birbhum, India. *Geoscience Frontiers* 8, 1105-
572 1114.

573 Veltri, M., Veltri, P., Maiolo, M., 1996. On the fractal description of natural channel networks. *Journal*
574 *of hydrology* 187, 137-144.

575 Wohl, E., Brierley, G., Cadol, D., Coulthard, T.J., Covino, T., Fryirs, K.A., Grant, G., Hilton, R.G., Lane,
576 S.N., Magilligan, F.J., 2019. Connectivity as an emergent property of geomorphic systems. *Earth*
577 *Surface Processes and Landforms* 44, 4-26.

578 Yadollahie, M., 2019. The flood in Iran: a consequence of the global warming? *The international*
579 *journal of occupational and environmental medicine* 10, 54.

580 Zadeh, L.A., 1965. Fuzzy sets. *Information and control* 8, 338-353.

581 Zaharia, L., Costache, R., Prăvălie, R., Ioana-Toroimac, G., 2017. Mapping flood and flooding potential
582 indices: a methodological approach to identifying areas susceptible to flood and flooding risk. Case
583 study: the Prahova catchment (Romania). *Frontiers of Earth Science* 11, 229-247.

584 Zhang, S., Guo, Y., Wang, Z., 2015. Correlation between flood frequency and geomorphologic
585 complexity of rivers network—a case study of Hangzhou China. *Journal of Hydrology* 527, 113-118.

586 Zhao, H., Guo, S., 2014. Selecting green supplier of thermal power equipment by using a hybrid MCDM
587 method for sustainability. *Sustainability* 6, 217-235.

588 Zhao, H., Guo, S., 2015. External benefit evaluation of renewable energy power in China for
589 sustainability. *Sustainability* 7, 4783-4805.

590 Zou, Q., Zhou, J., Zhou, C., Song, L., Guo, J., 2013. Comprehensive flood risk assessment based on set
591 pair analysis-variable fuzzy sets model and fuzzy AHP. *Stochastic Environmental Research and Risk*
592 *Assessment* 27, 525-546.

593

Figures

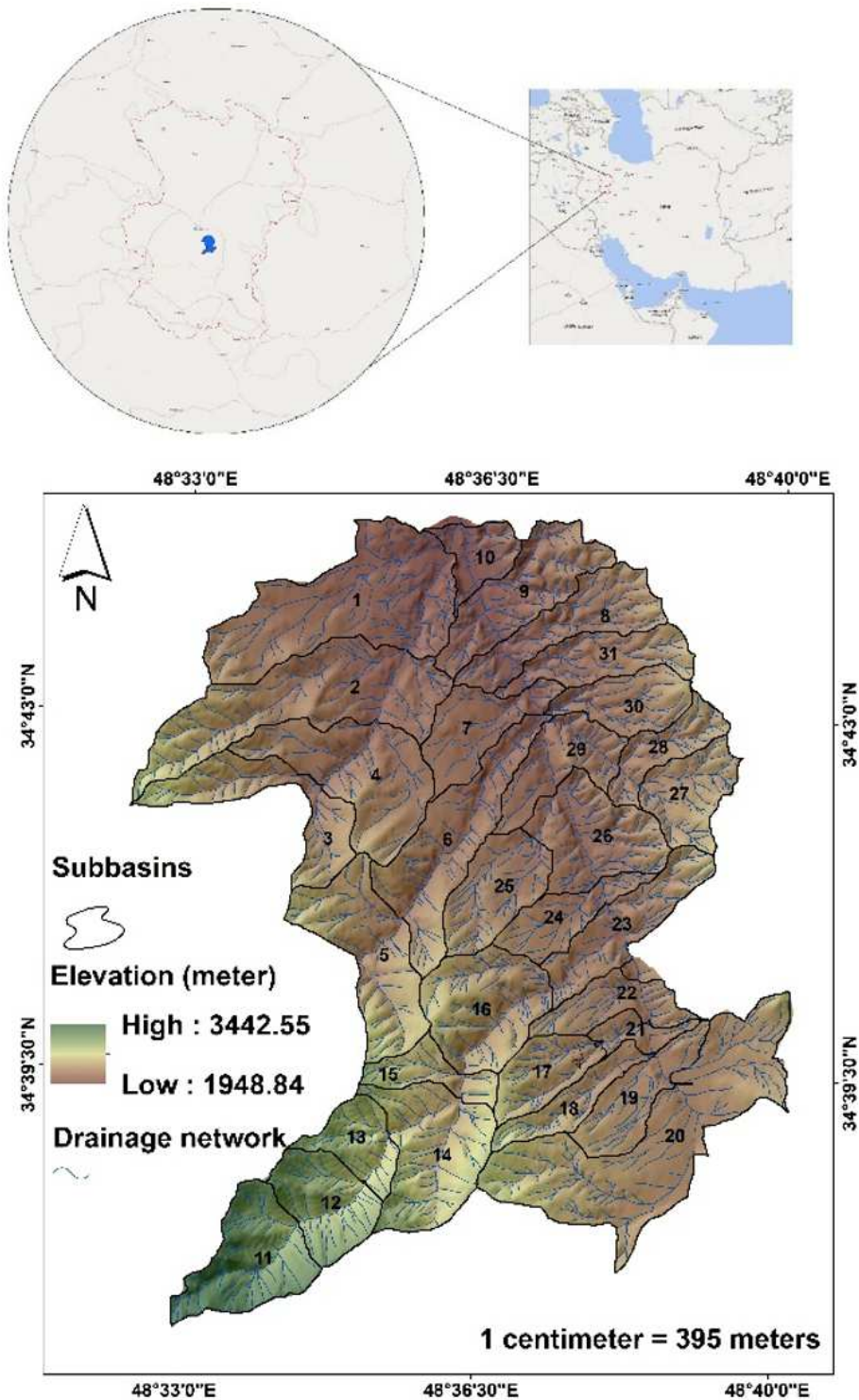


Figure 1

location of the case study Note: The designations employed and the presentation of the material on this map do not imply the expression of any opinion whatsoever on the part of Research Square concerning

the legal status of any country, territory, city or area or of its authorities, or concerning the delimitation of its frontiers or boundaries. This map has been provided by the authors.

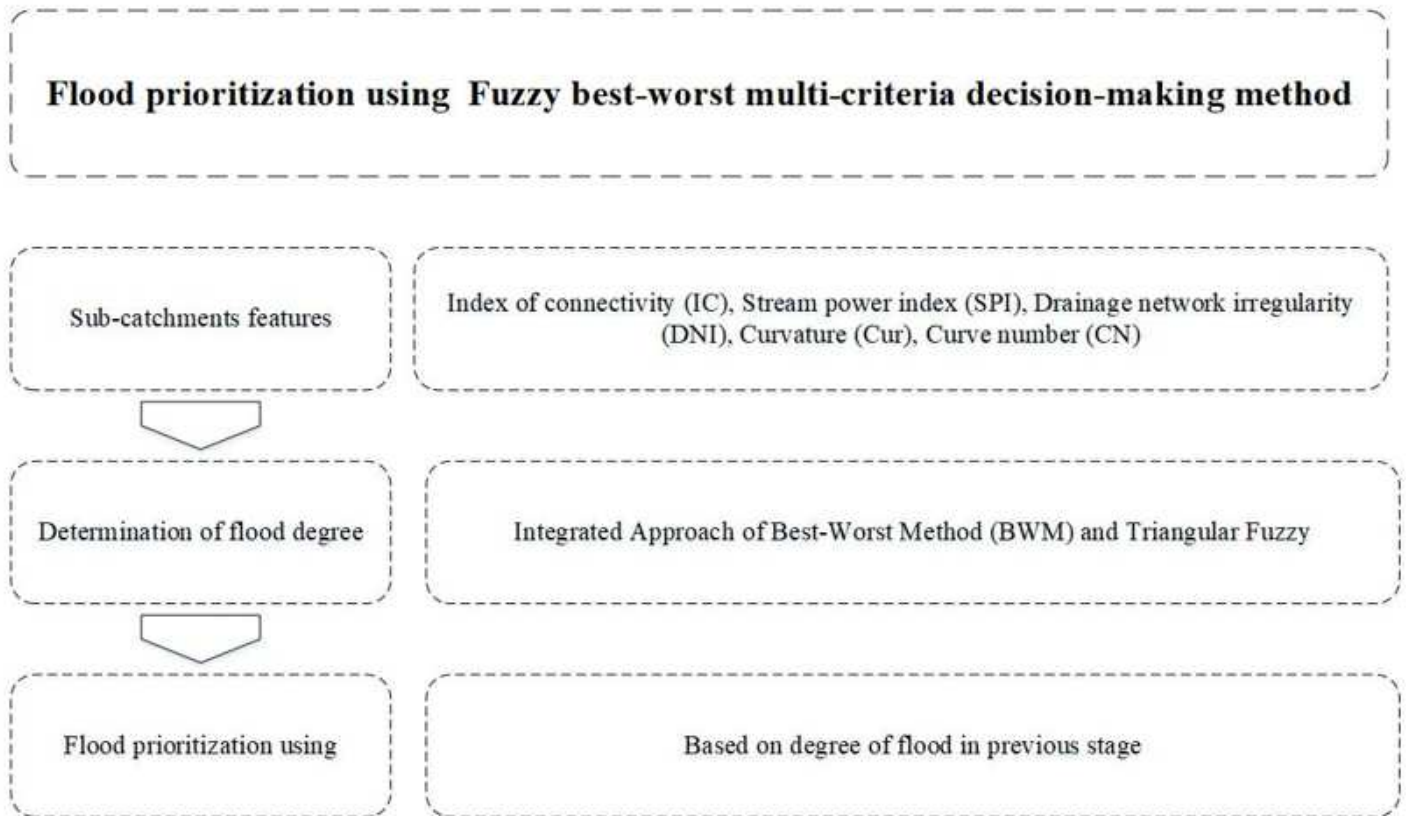


Figure 2

flowchart of the used methodology

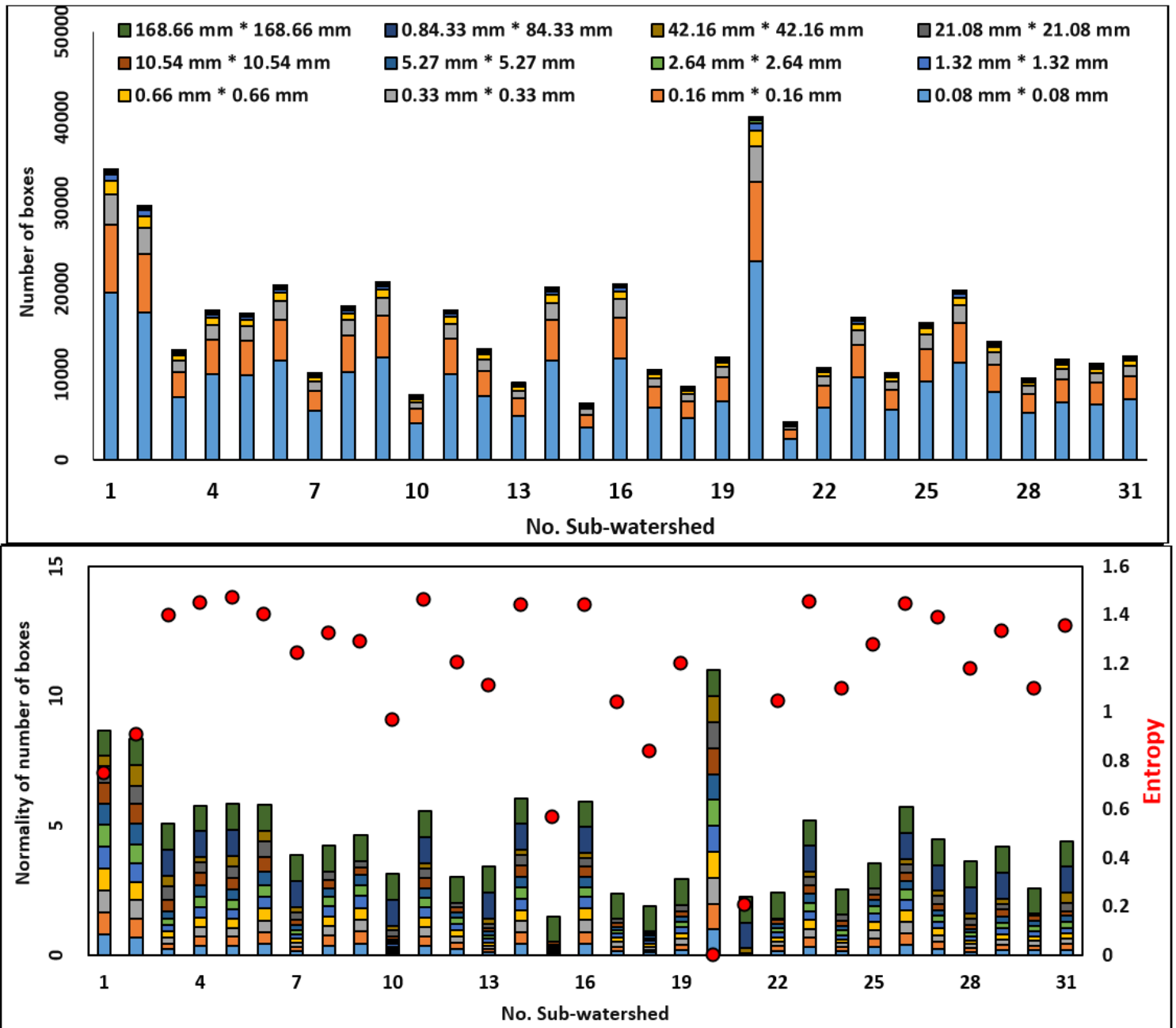


Figure 3

a: doing algorithm of box-counting method and, b: calculating EN based on box-counting method

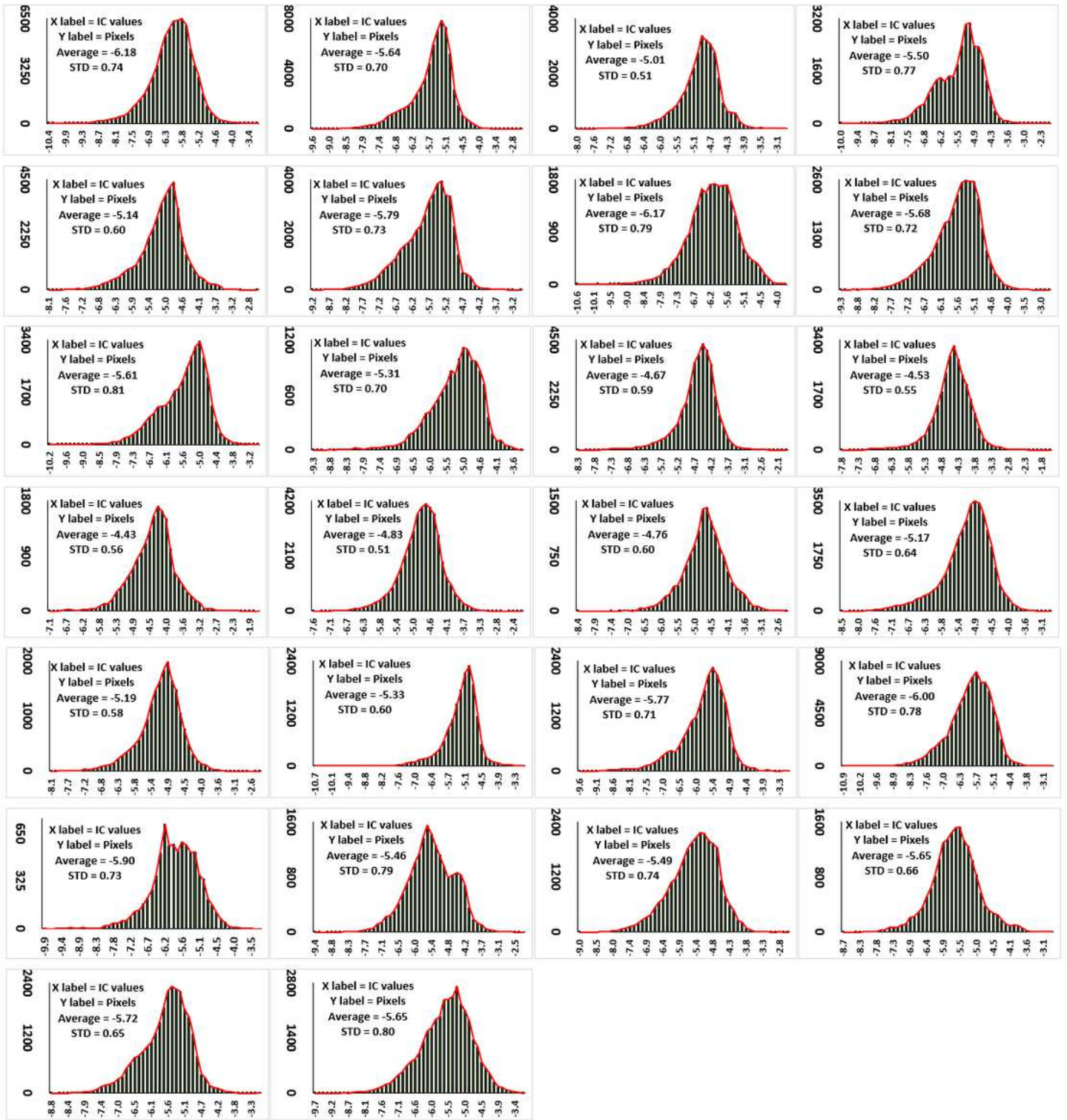


Figure 4

IC Values for sub-watersheds (Right to left is No. 1 to No. 31, respectively)

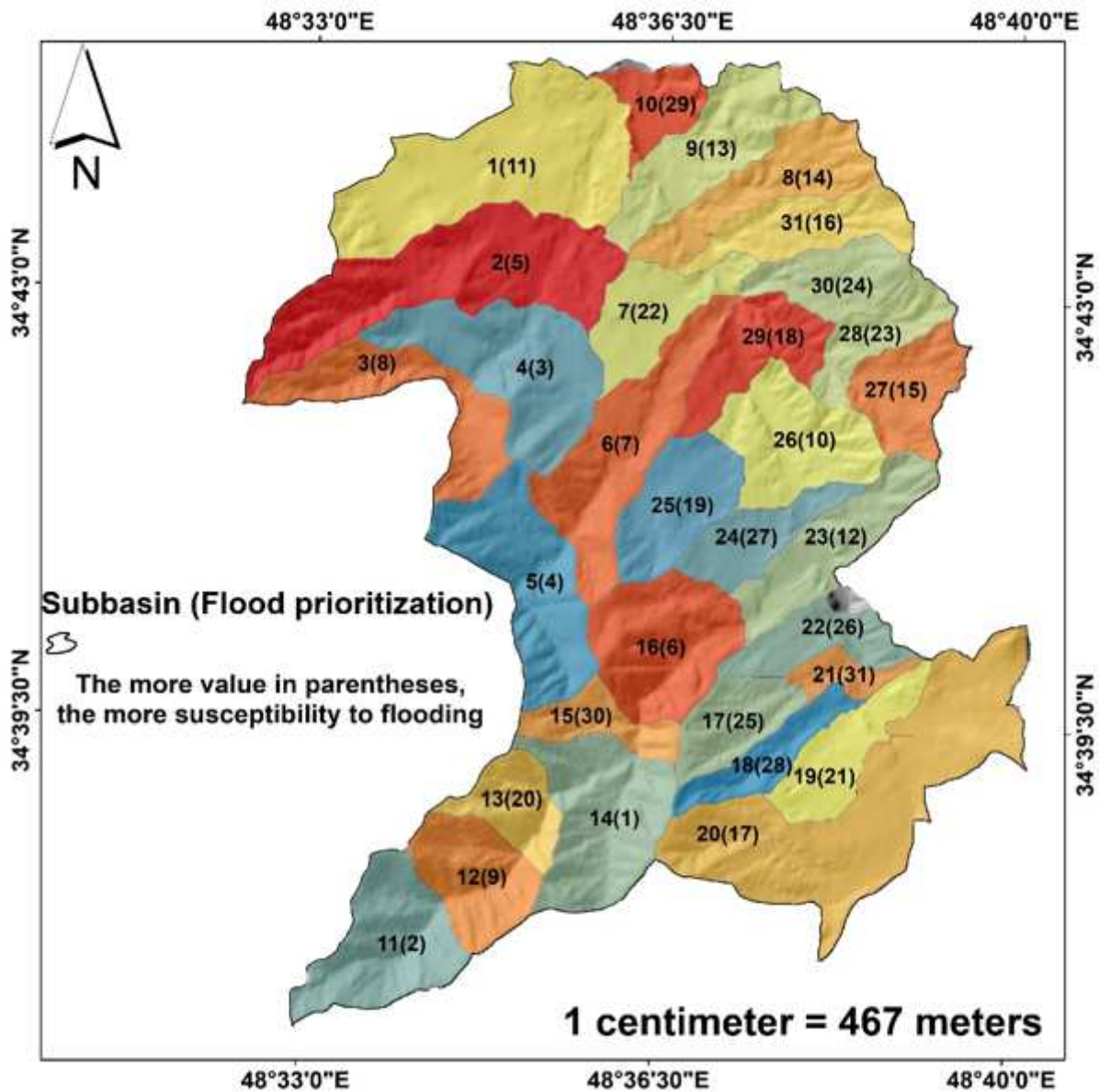


Figure 5

Flood prioritization of the case study Note: The designations employed and the presentation of the material on this map do not imply the expression of any opinion whatsoever on the part of Research Square concerning the legal status of any country, territory, city or area or of its authorities, or concerning the delimitation of its frontiers or boundaries. This map has been provided by the authors.